The Two NK-1 Binding Sites Correspond to Distinct, Independent, and Non-Interconvertible Receptor Conformational States As Confirmed by Plasmon-Waveguide Resonance Spectroscopy

Isabel D. Alves,*[,⊗,‡,§] Diane Delaroche,[||] Bernard Mouillac,[⊥] Zdzislaw Salamon,[‡] Gordon Tollin,[‡,§] Victor J. Hruby,[‡,§] Solange Lavielle,[||] and Sandrine Sagan[||]

Department of Biochemistry and Molecular Biophysics and Department of Chemistry, University of Arizona, Tucson, Arizona 85721, Université Pierre et Marie Curie-Paris6, UMR 7613, FR 2769, Paris F-75005, France, CNRS, UMR 7613, Paris F-75005, France, and Institut de Genomique Fonctionnelle, Departement de Genomique Fonctionnelle, CNRS UMR 5203 INSERM U661-Universite Montpellier I et II, 141 rue de la Cardonille, 34094 Montpellier Cedex 5, France

Received December 20, 2005; Revised Manuscript Received February 20, 2006

ABSTRACT: Two nonstoichiometric ligand binding sites have been previously reported for the NK-1 receptor, with the use of classical methods (radioligand binding and second messenger assays). The most populated (major, NK-1M) binding site binds substance P (SP) and is related to the adenylyl cyclase pathway. The less populated (minor, NK-1m) binding site binds substance P, C-terminal hexa- and heptapeptide analogues of SP, and the NK-2 endogenous ligand, neurokinin A, and is coupled to the phospholipase C pathway. Here, we have examined these two binding sites with plasmon-waveguide resonance (PWR) spectroscopy that allows the thermodynamics and kinetics of ligand−receptor binding processes and the accompanying structural changes of the receptor to be monitored, through measurements of the anisotropic optical properties of lipid bilayers into which the receptor is incorporated. The binding of the three peptides, substance P, neurokinin A, and propionyl[Met(O_2)^{11}]SP(7−11), to the partially purified NK-1 receptor has been analyzed by this method. Substance P and neurokinin A bind to the reconstituted receptor in a biphasic manner with two affinities ($K_{d1} = 0.14 \pm 0.02$ nM and $K_{d2} = 1.4 \pm 0.18$ nM, and $K_{d1} = 5.5 \pm 0.7$ nM and $K_{d2} = 620 \pm 117$ nM, respectively), whereas only one binding affinity ($K_d = 5.5 \pm 0.4$ nM) could be observed for propionyl[Met(O_2)^{11}]SP(7−11). Moreover, binding experiments in which one ligand was added after another one has been bound to the receptor have shown that the binding of these ligands to each binding site was unaffected by the fact that the other site was already occupied. These data strongly suggest that these two binding sites are independent and non-interconvertible on the time scale of these experiments (1−2 h).

Plasmon-waveguide resonance (PWR)[1] spectroscopy is an innovative experimental methodology that enables in-depth characterization of protein−protein, protein−lipid, and protein−ligand interactions occurring either within or at the surface of anisotropic thin films under native conditions and without the use of labels (*1*−*5*). No labeling is required since the analytical method is dependent on the intrinsic optical properties (refractive index, *n*, and optical absorption coefficient, *k*), as well as the thickness, *t*, of thin layers of material deposited onto the resonator surface. In this way, it is possible to detect as little as femtomole quantities of material. An important aspect is that PWR has the unique capability of independently examining changes in the *n*, *k*, and *t* values of a uniaxially oriented sample, such as a proteolipid film, both parallel and perpendicular to the membrane plane, in response to receptor−ligand interactions. As a result, one can monitor changes in the refractive index anisotropy in relation to long-range molecular order and molecular conformation changes occurring in the membrane upon protein functional activity (e.g., ligand binding) in an environment closely resembling the native state, i.e., a lipid bilayer (*6*). Moreover, PWR spectroscopy possesses several significant advantages compared to conventional surface plasmon resonance (SPR) methods. These include enhanced sensitivity and spectral resolution (due to narrower line widths) and the ability to distinguish between mass and conformational changes (*1*). The latter is a consequence of the ability of PWR to use both *p*- and *s*-polarized light excitation (electric vectors perpendicular and parallel to the membrane plane, respectively) to produce resonances and thereby to permit structural characterization (*7*), whereas SPR responds only to *p*-polarized excitation. By measuring plasmon resonances excited by both *s*- and *p*-polarized light, this technology

* To whom correspondence should be addressed. Telephone: 33 1 44 27 55 09. Fax: 33 1 44 27 71 50. E-mail: alves@ccr.jussieu.fr.

⊗ Present address: UMR 7613 CNRS-UPMC, case courrier 182, 4 place Jussieu, 75252 Paris cedex 05, France.

‡ Department of Biochemistry and Molecular Biophysics, University of Arizona.

§ Department of Chemistry, University of Arizona.

|| Université Pierre et Marie Curie-Paris6 and CNRS, UMR 7613.

⊥ CNRS UMR 5203 INSERM U661-Universite Montpellier I et II.

[1] Abbreviations: hDOR, human delta opioid receptor; NK-1, neurokinin 1; SP, substance P; PWR, plasmon-waveguide resonance; SPR, surface plasmon resonance; GPCR, G-protein-coupled receptor.

10.1021/bi052586d CCC: $33.50
Published on Web 03/30/2006

allows direct measurements of the anisotropic optical properties of biomembranes and real-time characterization of changes in the mass density and molecular orientation of molecules contained therein and thus can be used to monitor the thermodynamics and kinetics of binding processes and the accompanying structural changes.

In this study, we have incorporated the partially purified detergent-solubilized human neurokinin (NK-1) receptor into an egg PC lipid bilayer deposited onto the silica surface of a PWR resonator and have directly observed the ligand-induced conformational changes of the receptor. The NK-1 receptor belongs to the superfamily of GPCRs (G-protein-coupled receptors), more specifically to the rhodopsin-like subclass. This receptor is involved in a plethora of physiological processes in the cardiovascular, respiratory, gastrointestinal, immune, and nervous systems (*8*−*10*) through the action of the tachykinin family of peptides to which substance P (SP) belongs. There is evidence that SP also plays a role in pain modulation and neurogenic inflammation (*9*, *10*), and recent studies have associated this peptide with the pathogenesis of certain affective disorders (*11*). The receptor containing the FLAG M2 peptide at the N-terminus and a hexahistidine tag at the C-terminus was first stably expressed in CHO K1 cells and its pharmacological profile determined on the basis of the binding affinity and second messenger production assays. Three agonist peptides were particularly useful: substance P (SP, H-Arg-Pro-Lys-Pro-Gln-Gln-Phe-Phe-Gly-Leu-Met-NH_2), neurokinin A (NKA, H-His-Lys-Thr-Asp-Ser-Phe-Val-Gly-Leu-Met-NH_2), and a septide-like peptide, propionyl[Met(O_2)^{11}]SP(7−11) [the septide corresponds to [pGlu^6,Pro^9]SP(6−11) (*12*)]. Results were found to be similar to what had been previously reported for the wild-type receptor (*13*−*15*). For the PWR experiments, the interaction of the same peptide agonists with the receptor was investigated. For SP and NKA, two distinct binding processes were observed upon addition of increasing concentrations of ligand, which exhibit affinities comparable to what has been observed in classical radiolabeling pharmacological assays (*14*, *15*). In contrast, for propionyl[Met(O_2)^{11}]SP(7−11), only one binding process was observed (even when high concentrations of this ligand were used). The magnitudes, kinetics, and anisotropies of the conformational changes occurring upon binding of each ligand to the receptor were measured. Also, by addition of one ligand after the other to the receptor, the effect of having the receptor occupied by another ligand was investigated. The results obtained yield new insights about the nature of NK-1 binding sites and their activation mechanism and demonstrate that PWR provides a direct and alternative approach to investigating transmembrane signaling.

EXPERIMENTAL METHODS

Plasmon-Waveguide Resonance (PWR) Spectroscopy. Resonance spectra in this study were obtained using a Beta PWR instrument from Proterion (Piscataway, NJ) that records the relative reflectance (i.e., the ratio of reflected to incident light intensities) versus the absolute incident angle (α) of the exciting light with a resolution of 1 mdeg (millidegree). In our work, all PWR measurements were performed at 25 °C, which was kept constant within 0.1 °C throughout the experiment. It should be pointed out that independent PWR experiments generally yield different results in terms of the absolute positions of the spectra. This is due to a variety of factors, e.g., variations in the properties of the lipid bilayer and alterations of the resonator coating upon use. However, the magnitudes of the spectral shifts are reproducible and can be quantitatively compared from one experiment to another. The data presented in Tables 2 and 3 are the average of three independent experiments for which errors are shown. It should be noted that the scales (for both the *x*- and *y*-axes) used for *p*- and *s*-polarization data are different. This was done for practical reasons, since the resonance spectra obtained with *s*-polarization are sharper and shallower than those obtained with *p*-polarized light; thus, it is more convenient to use different scales.

The method is based upon the resonant excitation of collective electronic oscillations (plasmons) in a thin metal film (Ag), deposited on the external surface of a glass prism overcoated with a dielectric layer (SiO_2). Polarized light from a CW He−Ne laser (λ = 543.5 nm) is used under total internal reflection conditions. The resonant excitation of plasmons generates an evanescent electromagnetic field localized at the outer surface of the dielectric film, which interacts with molecules immobilized on this surface and can be used to probe their optical properties (*1*, *7*). It is important to point out that the plasmon exciting laser light is totally reflected from the external surface of the prism and therefore never reaches the sample located on the opposite side of the plasmon-generating film. Because the resonance coupling generates electromagnetic waves at the expense of incident light energy, the intensity of reflected light is diminished. The angular dependence of the reflectance corresponds to a PWR spectrum. Moreover, the resonance can be excited with light polarized with the electric vector either parallel (*s*) or perpendicular (*p*) to the membrane plane (which is opposite with respect to the incident plane), thereby allowing for characterization of the molecular organization of anisotropic systems such as biomembranes containing integral proteins (*1*, *2*).

The PWR spectra can be described by three parameters: spectral position, spectral width, and resonance depth. These experimental features depend on the optical and structural properties of the bilayer membrane, which are determined by the surface mass density (i.e., the amount of mass per unit surface area), the spatial mass distribution (i.e., the internal structure of the membrane, including molecular anisotropy and the long-range molecular order of the bilayer), the membrane thickness, and the absorption or light scattering properties of the membrane at the plasmon excitation wavelength. These optical properties are described by three parameters, the refractive index (*n*), the extinction (or scattering) coefficient (*k*), and the thickness (*t*) of the membrane, which can be evaluated by thin film electromagnetic theory based on Maxwell's equations (*1*, *16*). In this study, we are concerned only with the angular shifts and amplitudes of the resonance spectra, without any analysis using spectral fitting (*7*) or graphical analysis procedures (*17*). These spectral properties reflect the values of the refractive index and the thickness of the proteolipid layer, i.e., the mass density and spatial mass distribution related to the long-range molecular order and molecular conformation of the sample (*1*, *2*, *7*). For nonspherical molecules oriented uniaxially on the resonator surface, *n* values will be different for *s*- and *p*-polarization. This allows characterization of

anisotropy changes due to alterations in the molecular orientation and structure of the molecules in the proteolipid film (*7*).

Cell Culture. CHO cells were cultured in Ham's F-12 medium (Invitrogen) supplemented with 10% fetal bovine serum (Invitrogen), penicillin (100 units/mL) (Sigma), and streptomycin (100 mg/mL) (Sigma) in a humidified atmosphere containing 5% CO_2 at 37 °C.

Binding and Second Messenger Assays. These assays have been extensively described before (*13*−*15*). Briefly, for [^{3}H]-SP (120 Ci/mmol) binding assays, 5×10^3 cells per well were used, while 5×10^4 cells per well were needed for [^{3}H]propionyl[Met$(O_2)^{11}$]SP(7−11) (100 Ci/mmol) binding experiments (*13*−*15*). Time incubations at room temperature (22 °C) had durations of 100 and 80 min in Krebs-phosphate buffer (*13*−*15*). For second messenger experiments, CHO cells were seeded 48 h before being labeled for 24 h with [^{3}H]inositol (0.5 μCi per well) or [^{3}H]adenine (0.2 μCi per well) (*13*−*15*).

Receptor Solubilization and Purification. Confluent monolayers of CHO cells, grown in 15 cm dishes, were washed with Ham's F-12 basic medium and harvested using 5% trypsin in F-12. After centrifugation (2500 rpm for 20 min at 4 °C), the pellet was resuspended in 25 mM Tris-HCl (pH 7.4) containing protease inhibitors (1 mL/L) that are designed to be used with metal chelating columns (Sigma). Cell lysates were homogenized by 10 strokes with a tissue grinder. The homogenates were centrifuged at 42000*g* (Beckman Coulter, Fullerton, CA) for 30 min at 4 °C to remove nuclei and debris. Supernatants were aspirated, and the membrane-enriched pellets containing the NK-1 receptor were resuspended in solubilization buffers 25 mM HEPES, 30 mM octyl glucoside (Sigma), 0.5 M KCl, and protease inhibitors (1 mL/L). The membranes were then homogenized with 15 strokes and centrifuged at 42000*g* (Beckman Coulter). This allowed the separation of a small amount of insoluble material from the supernatant. The supernatant was added to a nickel chelating resin (His-Select HC nickel affinity gel; Sigma) (0.5 mL of resin per gram of lysed cells) in a 10 mL polypropylene column (Pierce, Rockford, IL) pre-equilibrated with the solubilization buffer mentioned above and placed on a rocker platform for 1 h at 4 °C. The resin was incubated first (20 min) with the detergent buffer containing 30 mM imidazole followed by the same procedure but with 60 mM imidazole to remove nonspecifically bound proteins. The resin was then washed once with 3 column volumes of solubilization buffer followed by elution with the same buffer containing 100 mM imidazole [a similar procedure has been used in the purification of the hDOR (*5*)]. The purity of the receptor preparation was assessed using a 10% SDS electrophoresis gel which was developed with silver staining. The gel exhibited mainly two bands, one around 60 kDa that should correspond to the post-translational modified form of the receptor and the other of approximately twice this mass that may correspond to a dimer of this receptor or to a contaminant protein (see the Supporting Information). It should be pointed out that the receptor was not extensively purified in these studies. As discussed below, the existence of contaminant proteins in the receptor preparation does not interfere with the PWR signal as one measures the ligand-induced receptor conformational changes, and so, the only protein in the system that responds to ligand is the NK-1 receptor. A Western blot was performed in which a mouse anti-$(His)_5$ antibody (Qiagen) was used followed by an Immun-Star chemiluminescent protein detection system (Bio-Rad). Proteins were visualized on X-OMAT photographic films (Kodak). A bicinchoninic acid assay was performed to determine the protein concentration in the sample (Pierce). The purple reaction product was monitored at 560 nm using an enzyme-linked immunosorbent assay plate reader (μQuant; Bio-Tek Instruments, Winooski, VT). Approximately 100 μg of protein was obtained after affinity purification when 20 plates (15 cm diameter) of cells grown to confluence were harvested. The biological activity of the solubilized and purified receptor was not measured by classical radioligand binding assays but rather analyzed with PWR by the capacity of the ligand to bind to the receptor with affinities similar to what has been published in the literature using competition assays with radiolabeled ligands. It has been reported by several laboratories that the affinity of the receptor for its ligand varies depending on the receptor environment (lipid vs detergent). Measuring the receptor biological activity in the lipid bilayer, as performed in this study, is advantageous because the system mimics better the receptor biological environment and gives binding affinities similar to those obtained using native membrane preparations.

Lipid Bilayer Formation and Receptor Incorporation. In this study, we used self-assembled solid-supported lipid membranes (*1*). The method of preparation uses the same principles that govern the spontaneous formation of a freely suspended lipid bilayer membrane (called a black lipid membrane) (*18*). Briefly, bilayer generation involves the spreading of 2 μL of a lipid solution [7 mg/mL egg phosphatidylcholine (Avanti Polar Lipids) in a squalene/butanol/methanol mixture (0.05:9.5:0.5, v/v)] across a small orifice in a Teflon spacer which separates the silica waveguide surface from the aqueous phase [10 mM Tris-HCl containing 0.5 mM EDTA and 10 mM KCl (pH 7.3)] in the PWR cell (*1*). The hydrophilic SiO_2 surface is covered with a thin layer of water of condensation (*19*, *20*) and attracts the polar groups of the lipid molecules with the hydrocarbon chains oriented toward the bulk lipid phase, which induces an initial orientation of the lipid molecules. The next step involves addition of aqueous buffer to the sample compartment of the PWR cell, which results in formation of an annular plateau−Gibbs border of lipid solution that anchors the membrane to the Teflon spacer. This border allows membrane flexibility wherein the bilayer can deform and lipid molecules can become displaced or recruited upon insertion of a membrane protein or as a result of ligand-induced protein conformational changes. This produces a lipid bilayer with a thickness of ∼5.5 nm, including the hydrated lipid headgroups (*21*) (before the incorporation of receptor).

The incorporation of the human NK-1 receptor into this lipid bilayer was accomplished by introducing the purified and detergent-solubilized receptor into the aqueous compartment under conditions that dilute the detergent to below the critical micelle concentration, which allows the membrane protein to spontaneously incorporate into the lipid bilayer. The system equilibrated (no further shifts observed in the spectra) in ∼1−2 h, after which the cell sample was washed with buffer to remove loosely bound receptor molecules. This process usually led to a small shift (when compared with

the total shift upon receptor incorporation given below) in the PWR spectra (~5−10 mdeg) to smaller angles, after which it stabilizes. It should be pointed out that the addition of the buffer system used for the solubilization of the receptor to the PWR cell sample after bilayer deposition did not produce changes in the PWR spectra. Experiments have been performed (T. Georgieva, personal communication) with CHO cells (K1 cell line; the same used to express the NK-1 receptor) expressing no receptor, and no significant shifts in the spectra were produced when membrane homogenates from this cell line were added to the PWR cell sample after bilayer deposition, showing that other proteins that may be copurified with the receptor did not insert in the lipid bilayer. Further addition of ligands to the above-described system also produced no changes in the spectra, also demonstrating that the small quantities of contaminant protein in the PWR experiments did not interfere with the spectral changes observed upon the ligand-induced receptor conformational changes described below.

Addition of Ligand to the Proteolipid System. Between 20 and 100 μL of ligand {SP, NKA, and propionyl[Met(O_2)^{11}]-SP(7−11)} dissolved in the above-mentioned buffer system was added to the cell sample such that after dilution in the cell chamber, the target concentration was achieved. The first concentration point was chosen to be approximately 1 order of magnitude lower than the published value of the dissociation constant (K_d) for that ligand. Incremental amounts of ligand were then added in a cumulative fashion, and the PWR spectra were acquired for each point when equilibrium was reached (i.e., when no further changes in the PWR spectra occurred; this required ~10 min for the first binding process and less than 1 min for the second one). K_d values were obtained by plotting the resonance minimum position for the PWR spectra as a function of ligand concentration and fitting to the hyperbolic function that describes the 1:1 binding of a ligand to a receptor using GraphPad Prism (GraphPad Software). Since the spectral shifts were directly proportional to the amount of ligand bound and this quantity was much smaller than the total amount of ligand added, this analysis resulted in a thermodynamically valid binding constant (see below).

RESULTS

The human NK-1 receptor containing the two labels at the N-terminus (Flag M2) and C-terminus (hexaHis) of its sequence has been cloned in CHO K1 cells. The clone used herein expressed high levels of the receptor. Saturation binding studies were done with [^{3}H]SP that binds at the two NK-1 binding sites and with [^{3}H]propionyl[Met(O_2)^{11}]SP-(7−11) that is selective for the less populated NK-1m binding site (*14*). Moreover, as reported for the wild-type receptor (*14*), only one binding affinity could be determined for the two radioligands (Table 1). The maximal binding parameters (B_{max}) differ for the two radioligands, the one corresponding to [^{3}H]propionyl[Met(O_2)^{11}]SP(7−11) being 17% of the receptor population bound by [^{3}H]SP. Competition binding studies (not shown) with SP, NKA, and propionyl[Met(O_2)^{11}]-SP(7−11) with one or the other radioligands confirmed that [^{3}H]SP mostly binds to the major binding site (NK-1M) for which SP is a high-affinity competitor, while NKA and propionyl[Met(O_2)^{11}]SP are low-affinity binders. On the other hand, all three peptides are high-affinity competitors for the minor NK-1m binding site (data not shown) selectively labeled with [^{3}H]propionyl[Met(O_2)^{11}]SP(7−11). As the NK-1M and NK-1m binding sites have been related to adenylyl cyclase and phospholipase C activation, respectively (*13*, *14*, *22*, *23*), the potency of SP, NKA, and propionyl[Met(O_2)^{11}]-SP(7−11) in stimulating the two intracellular metabolic pathways has been evaluated (Table 2). As expected, all three peptides are potent agonists with respect to accumulation of IP second messenger, while only SP is efficient in stimulating cAMP (Table 2).

Table 1: Pharmacological Analysis of the FLAG M2-hNK-1-(His)$_6$ Receptor Stably Expressed in CHO K1 Cells[a]

radiolabeled peptide	K_d (nM)	B_{max} (fmol/mg of protein)
[^{3}H]substance P (NK-1M site)	1.3 ± 0.1	9400 ± 600
[^{3}H]propionyl[Met(O_2)^{11}]SP(7−11) (NK-1m site)	4.3 ± 0.2	1600 ± 320

[a] The radioligands recognize either one (NK-1m), [^{3}H]propionyl-[Met(O_2)^{11}]SP(7−11), or both (NK-1m and NK-1M), [^{3}H]SP, NK-1 binding sites. However, according to the cell number (5000 cells per well), the specific binding of [^{3}H]SP is to only NK-1M sites (*9*). Binding parameters (dissociation constants, K_d, and maximal ligand bound, B_{max}) were determined on membrane homogenates. The NK-1M and NK-1m binding sites had previously been shown to be related to cAMP and IP accumulation, respectively (Table 2).

Table 2: Pharmacological Analysis of the FLAG M2-hNK-1-(His)$_6$ Receptor Stably Expressed in CHO K1 Cells[a]

	second messenger production EC_{50} (nM)		
second messenger pathway	substance P	NKA	propionyl[Met(O_2)^{11}]-SP(7−11)
cAMP (NK-1M)	11 ± 6	1000 ± 350	>5000
IP (NK-1m)	3.0 ± 0.5	2.2 ± 0.8	11 ± 7

[a] Potencies of SP, NKA, and propionyl[Met(O_2)^{11}]SP(7−11) in stimulating the accumulation of cAMP or IP were measured on whole CHO cells. The NK-1M and NK-1m binding sites had previously been shown to be related to cAMP and IP accumulation, respectively.

With regard to PWR experiments, NK-1 receptor molecules were incorporated into a preformed lipid bilayer deposited on the hydrophilic silica surface (see Experimental Methods for details) by addition of small aliquots of a concentrated solution of protein (200 nM being the total added concentration of the protein after dilution in the cell sample compartment) dissolved in 30 mM octyl glucoside detergent-containing buffer to the aqueous volume of the cell sample. This process dilutes the detergent to below the critical micelle concentration (25 mM for octyl glucoside), resulting in a spontaneous transfer of receptor molecules from micelles to the bilayer. It should be noted that not all receptor molecules that are added to the PWR cell sample are inserted into the lipid bilayer. Indeed, previous studies performed with the hDOR, where the amount of receptor in the lipid bilayer was determined, have shown that only ~5% of the receptor that is added to the cell sample is incorporated into the bilayer (*24*). It has also to be mentioned that the receptor preparation is quite pure and does not contain detectable receptor-interacting proteins, such as G-proteins as observed by SDS gel electrophoresis (see the Supporting Information). It should be pointed that we do not know the directionality of incorporation of the receptor into the lipid bilayer. As was observed with the hDOR (*5*) which belongs to the same subclass of GPCRs as the NK-1, we presume that the receptor

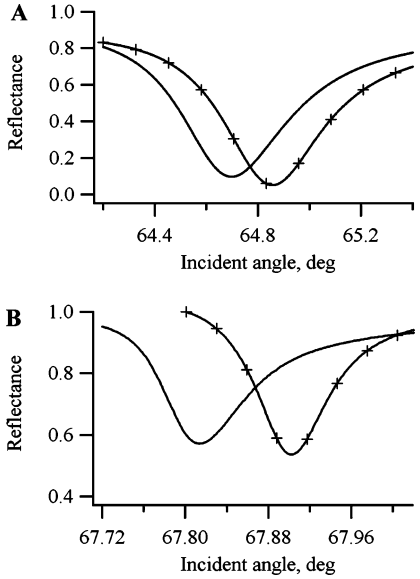

FIGURE 1: PWR spectra representing the incorporation of the human NK-1 receptor into an egg PC solid-supported lipid bilayer. Panels A and B show the spectra for the lipid bilayer before (solid line) and after (solid line with + symbols) receptor incorporation (the final receptor concentration in the PWR sample cell was approximately 200 nM) obtained with *p*-polarized (A) and *s*-polarized (B) light, respectively.

is bidirectionally oriented, with either the ligand-binding site or the G-protein binding site facing the aqueous compartment of the PWR sample cell. As can be seen in panels A and B of Figure 1, the incorporation of the receptor into the lipid bilayer produced a shift to higher angles for both *p*- and *s*-polarized light (in the interpretation of this, differences in the *x*-axis scale should be taken into account). These are related to increases in the refractive index due to an increase in the deposited mass on the resonator surface, as well as to increases in the proteolipid film thickness. The shifts produced upon receptor incorporation were larger for *p*-polarization than for *s*-polarization (~150 mdeg for *p*-polarization vs ~90 mdeg for *s*-polarization). This is characteristic of an anisotropic structural change, as was also observed previously in studies with the hDOR (*5*) and rhodopsin (*24*), consistent with the cylindrical shape of the receptor which is uniaxially oriented within the lipid bilayer (i.e., long axis oriented perpendicular to the lipid bilayer), rather than just randomly adsorbed to the bilayer surface, clearly reflecting a corresponding increase in the average long range molecular order and the thickness of the membrane resulting from receptor−lipid interactions. The receptor incorporation also produced changes in the depth of the spectra, which are also due to these interactions. The lipid bilayer thickness is expected to increase upon receptor incorporation with the hydrophobic portion of the protein localizing within the bilayer interior and the peripheral portions of the protein extending outside the membrane on each side of the bilayer. To quantify these effects, spectral fitting procedures have to be utilized, which are beyond the scope of this work. However, the results are qualitatively consistent with expectations.

Changes in the PWR spectra caused by ligand−receptor interactions are shown in Figures 2−4. These also reflect alterations in the *n* and *t* values (*k* values different than zero result only from scattering effects, inasmuch as the PWR excitation wavelength is not absorbed by any of the sample components) resulting from mass increases and/or changes in conformation (*4*, *21*). In control experiments, the ligands were added to the lipid bilayer (in the absence of receptor) and no appreciable shifts were observed in the PWR signal.

The qualitative aspects of the spectral changes associated with the interaction of each of the ligands {SP, NKA, and propionyl[Met(O_2)^{11}]SP(7−11)} with the NK-1 receptor reconstituted in the lipid bilayer are described in Figures 2−4. As can be seen in panels A and B of these figures, the interaction of the ligand with the proteolipid system resulted

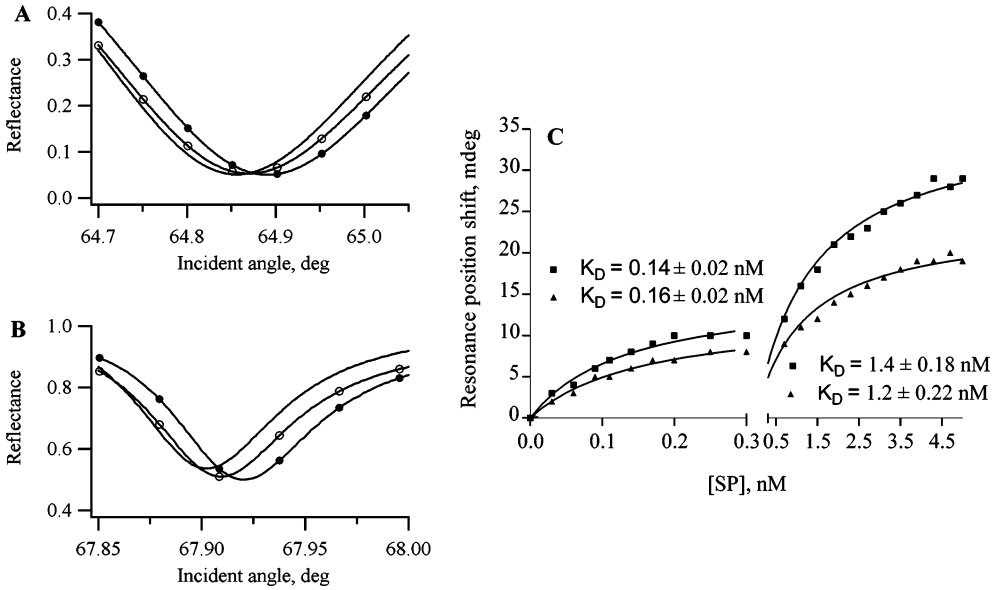

FIGURE 2: PWR spectra obtained after incremental addition of SP to the NK-1 receptor reconstituted into the lipid bilayer. Panels A and B represent the spectra obtained after incorporation of the NK-1 receptor into the lipid bilayer (solid line) and after the addition of 0.3 nM (solid line with ○ symbols) and 5 nM (solid line with ● symbols) of SP obtained with *p*- and *s*-polarized light, respectively. Panel C represents the binding curves obtained for the incremental addition of SP to the receptor, obtained with *p*-polarized (■) and *s*-polarized (▲) light. The total spectral shifts observed are presented in Table 3. The solid lines indicate single hyperbolic fits to the data with dissociation constant (K_d) values given in Table 4.

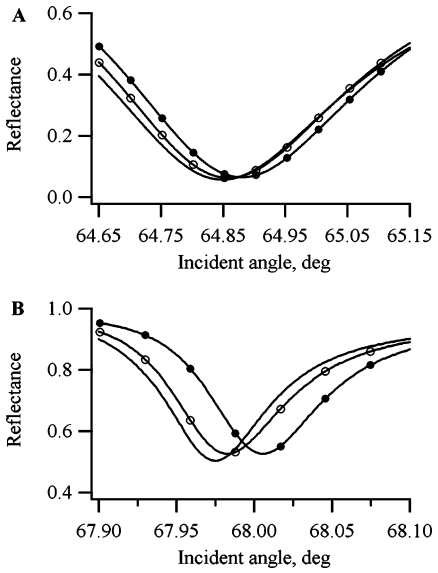

FIGURE 3: PWR spectra obtained after incremental addition of NKA to the NK-1 receptor reconstituted into the lipid bilayer. Panels A and B represent the spectra obtained after incorporation of the NK-1 receptor into the lipid bilayer (solid line) and after the addition of 10 nM (solid line with ○ symbols) and 6 μM (solid line with ● symbols) of NKA, obtained with *p*- and *s*-polarized light, respectively. The total spectral shifts observed are presented in Table 3. K_d values are given in Table 4.

in shifts in the spectra to larger angles for both *p*- and *s*-polarized light and for both concentration ranges that were investigated {note that for propionyl[Met(O_2)^{11}]SP(7−11) only one binding event was observed}. These are a result of both receptor and lipid bilayer conformation changes that are induced by the ligand binding to the receptor. It is particularly interesting to note that the shifts produced in the first binding event for the SP and NKA ligands are mostly isotropic (shifts in the *p*- and *s*-polarized light are similar in magnitude) and are small (9−10 mdeg for *p*-polarization and 8−9 mdeg for *s*-polarization); the second event produces anisotropic spectral shifts (shifts for *p*-polarization are larger than those for *s*-polarized excitation), and the spectral changes are larger in magnitude (19−23 mdeg for *p*-polarization and 11−17 mdeg for *s*-polarization) (panel C of Figures 2 and 4 and Table 3). These results indicate that the different concentrations of ligand produced different structural changes in the proteolipid system that corresponds to different receptor conformational states. It is also possible that the different magnitudes of the spectral changes observed for the two binding events could be ascribed to different ratios of two receptor isoforms, one that would bind the ligand at a low concentration and the other at a high concentration. However, the different anisotropies would still require that the structural changes produced by these two isoforms be different. The kinetics of the conformational changes associated with the two binding events were also quite different, the first binding process being slower (reaching equilibrium in ∼20 min) than the second one, which occurred in seconds (40−50 s to reach equilibrium).

By plotting the PWR spectral shifts obtained for the incremental additions of ligand, one obtains hyperbolic curves that can be fit to obtain the K_d value for the interaction of the ligand with the receptor (panel C of Figures 2 and 4).

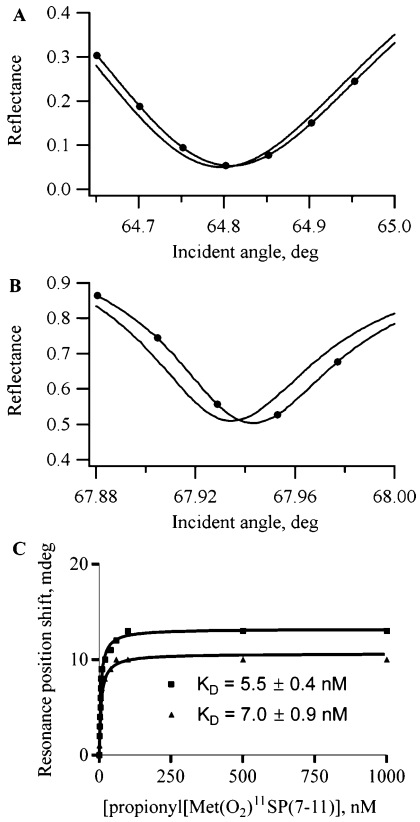

FIGURE 4: PWR spectra obtained after incremental addition of propionyl[Met(O_2)^{11}]SP(7−11) to the NK-1 receptor reconstituted into the lipid bilayer. Panels A and B represent the spectra obtained after incorporation of the NK-1 receptor into the lipid bilayer (solid line) and after the addition of a maximum concentration of 1 μM (solid line with ● symbols) propionyl[Met(O_2)^{11}]SP(7−11) obtained with *p*- and *s*-polarized light, respectively. Panel C represents the binding curves obtained for the incremental addition of propionyl-[Met(O_2)^{11}]SP(7−11) to the receptor obtained with *p*-polarized (■) and *s*-polarized (▲) light. The total spectral shifts observed are presented in Table 3. The solid lines indicate single hyperbolic fits to the data with K_d values given in Table 4.

It is important to note that, in these experiments, we do not directly determine the concentrations of the receptor and ligand in the PWR cell. Affinities are determined on the basis of the PWR spectral changes that occur due to mass increases and structural transitions in the proteolipid system upon incremental addition of ligand to the sample cell. Only material that is deposited on the resonator surface affects the PWR signal; i.e., there is no interference from the material that is in the bulk solution. Thus, the spectral changes are proportional to the amount of ligand bound to the receptor, and plots of spectral shifts versus bulk ligand concentration allow a direct determination of binding affinity. In other words, each concentration point in a saturation curve corresponds to the total ligand added to the aqueous compartment versus the amount bound, and it is assumed that the bulk material is able to freely diffuse and equilibrate with the membrane. The K_d values obtained here (Table 4) correlate well with the ones obtained using pharmacological assays (*14*, *15*), showing that the receptor was biologically functional and that the PWR spectral shifts represent receptor conformational changes that occur upon ligand binding and are not dictated by the presence of specific G-proteins.

In the case of propionyl[Met(O_2)^{11}]SP(7−11) binding to the receptor, only one binding curve was observed, even

Table 3: Resonance Position Shifts Observed upon Binding of Ligand to NK-1 by PWR Spectroscopy[a]

Entry	Ligand	Resonance position shift (mdeg)			
		p-pol.	*s*-pol.	*p*-pol.	*s*-pol.
1	Substance P (SP)	$[0.3\ nM]_{max}$		$[5\ nM]_{max}$	
		10	8	19	11
2	Neurokinin A (NKA)	$[10\ nM]_{max}$		$[6000\ nM]_{max}$	
		9	8	23	17
3	propionyl[Met$(O_2)^{11}$]SP(7-11)	$[1000\ nM]_{max}$			
		13	10	only one binding curve	
4	SP 1st/ NKA 2nd	two binding curves for SP NKA had no effect			
5	SP 1st propionyl[Met$(O_2)^{11}$]SP(7-11) 2nd	two binding curves for SP propionyl[Met$(O_2)^{11}$]SP(7-11) had no effect			
6	NKA 1st SP 2nd	NKA $[40\ nM]_{max}$ one binding curve		SP $[3\ nM]_{max}$ one binding curve	
		10	9	19	12
7	NKA 1st propionyl[Met$(O_2)^{11}$]SP(7-11) 2nd	NKA $[1000\ nM]_{max;}$ two binding curves propionyl[Met$(O_2)^{11}$]SP(7-11) had no effect			
8	propionyl[Met$(O_2)^{11}$]SP(7-11)1st SP 2nd	propionyl[Met$(O_2)^{11}$]SP(7-11) $[1000\ nM]_{max}$ one binding curve		SP $[3\ nM]_{max}$ one binding curve	
		12	10	20	10
9	propionyl[Met$(O_2)^{11}$]SP(7-11)1st NKA 2nd	propionyl[Met$(O_2)^{11}$]SP(7-11) $[1000\ nM]_{max}$ one binding curve		NKA $[1000\ nM]_{max}$ one binding curve	
		11	10	24	16

[a] Results for one ligand were obtained with the ligand alone or after binding of a second ligand to observe possible effects of the first ligand on the binding of the second. The results were obtained from three independent experiments; errors are ±1 mdeg.

when the concentration of ligand was increased up to 1 μM (3 orders of magnitude above the K_d reported for this ligand), suggesting that only one conformational state is induced in the receptor. This could mean that only one of the two binding sites was being occupied or that both sites were occupied with similar affinities and similar spectral changes. The second possibility is however ruled out since pharmacological studies have shown that this ligand binds with high affinity to only one of the binding sites (*14*, *15*). Again the observed K_d value (Table 4) was comparable to the one reported in the literature (*14*, *15*). In addition, the magnitude of the conformational changes was comparable to the ones observed for the low-concentration binding curves (corresponding to binding to the minor binding site, NK-1m) of both SP and NKA (Table 3). The kinetics of binding of propionyl[Met$(O_2)^{11}$]SP(7−11) to the receptor was slow (equilibrium was reached in approximately 20 min), again comparable to that observed with the lower-concentration binding event of both SP and NKA. These correspondences suggest, but do not prove, that the NK-1m site is the one being occupied by this ligand.

To test the effect of the presence of one ligand on the binding process and receptor conformational change of another, one ligand was added at low concentrations to the receptor (to occupy only one of the binding sites) and the PWR spectral changes were monitored. The second ligand was then added, and again the process was followed. In all cases, the presence of the first ligand did not measurably affect the binding process of the second, in terms of both the net spectral shifts observed (Table 3) and the binding affinities (Table 4), as well as kinetically (data not shown). The results indicate that the two binding sites are independent and non-interconvertible, at least in the time domain of the experiment (1−2 h).

DISCUSSION

Despite numerous studies, both physiologically and in a recombinant system, the unusual pharmacological behavior of the NK-1 receptor is still puzzling (*26*−*29*). In particular, pharmacological studies in this laboratory have shown that two distinct binding sites exist in this receptor (*13*, *14*). The major binding site, NK-1M, binds substance P that has been

Table 4: Affinities between Ligands and the NK-1 Receptor As Determined by PWR Spectroscopy[a]

Entry	Ligand	Kd (nM)			
		p-pol.	*s*-pol.	*p*-pol.	*s*-pol.
1	Substance P (SP)	[0.3 nM]$_{max}$		[5 nM]$_{max}$	
		0.14 ± 0.02	0.16 ± 0.02	1.4 ± 0.18	1.2 ± 0.22
2	Neurokinin A (NKA)	[10 nM]$_{max}$		[6000 nM]$_{max}$	
		5.5 ± 0.7	5.7 ± 1	620 ± 117	574 ± 166
3	propionyl[Met(O_2)^{11}]SP(7-11)	[1000 nM]$_{max}$			
		5.5 ± 0.4	7 ± 0.9	Only one binding curve	
4	SP 1st NKA 2nd	two binding curves for SP with similar Kd's as in entry 1 NKA had no effect			
5	SP 1st propionyl[Met(O_2)^{11}]SP(7-11)2nd	two binding curves for SP with similar Kd's as in entry 1 propionyl[Met(O_2)^{11}]SP(7-11) had no effect			
6	NKA 1st SP 2nd	NKA [40 nM]$_{max}$ one binding curve		SP [3 nM]$_{max}$ one binding curve	
		5.7 ± 0.9	5.6 ± 0.8	1.3 ± 0.2	1.2 ± 0.23
7	NKA 1st propionyl[Met(O_2)^{11}]SP(7-11) 2nd	NKA [1000 nM]$_{max}$; two binding curves with similar Kd's as in entry 2 propionyl[Met(O_2)^{11}]SP(7-11) had no effect			
8	propionyl[Met(O_2)^{11}]SP(7-11) 1st SP 2nd	propionyl[Met(O_2)^{11}]SP(7-11) [1000 nM]$_{max}$ one binding curve with similar Kd's as in entry 3		SP [3 nM]$_{max}$ one binding curve	
				1.4 ± 0.24	1.3 ± 0.21
9	propionyl[Met(O_2)^{11}]SP(7-11) 1st NKA 2nd	propionyl[Met(O_2)^{11}]SP(7-11) [1000 nM]$_{max}$ one binding curve with similar Kd's as in entry 3		NKA [1000 nM]$_{max}$ one binding curve	
				635 ± 132	601 ± 148

[a] The maximum ligand concentration added is shown in each case. In some experiments, a second ligand was added after the first one to determine if binding occurred. The results were obtained from three independent experiments, and errors are given.

shown to activate adenylyl cyclase. The minor binding site, NK-1m, also binds substance P, as well as neurokinin A, the endogenous NK-2 ligand, and is responsible for the activation of phospholipase C. These two binding sites are not present in stoichiometric quantities, the major NK-1M site predominating both in the rat submandibular glands and in CHO cell lines stably transfected with the human NK-1 receptor (*14*). The septide-like ligand was demonstrated to bind selectively to the minor site (*14*) and was used here to investigate possible conformational interconversion between the two binding sites induced by the ligand (*15*).

The PWR studies presented here provide information about the conformational changes and affinities associated with ligand binding to each receptor binding site. The data show that the conformational change induced by ligand binding to each site, in the absence of G-protein and intracellular machinery, is distinctly different. Specifically, the conformational change produced by occupancy of the minor site is smaller and isotropic and that produced by occupancy of the major site is larger and anisotropic. The kinetics associated with each binding site was also found to be distinct, the minor site conformational change being slower (on the order of minutes) than the major site conformational change (on the order of seconds). The experiments involving binding of one ligand after the other has been bound to the receptor show that the binding of ligand to each binding site is unaffected by the fact that the other has already been occupied. These data indicate that the two binding sites are associated with different conformations of the receptor and are totally independent and non-interconvertible, at least on the time scale of the experiment. In addition, non-PWR kinetic, saturation, and competition studies performed using [^{3}H]propionyl[Pro^9]SP also have demonstrated the existence of two independent binding sites that are non-interconvertible (*15*). The results obtained here not only confirm the studies mentioned above but also extend these by providing valuable information about the properties of the distinct conformational states observed in the receptor in terms of both their magnitude and anisotropies.

The use of a model system in our studies, compared to the in vivo system described above, consisting of a receptor reconstituted into a lipid bilayer where G-proteins and other

proteins are absent, also provides valuable information regarding the basis for the existence of the two binding sites. Specifically, our studies demonstrate that the existence of two binding sites in this receptor is an inherent property of the receptor and not a result of preferential coupling of this receptor with a particular protein (e.g., G-protein) as previous pharmacological data indicated (*14*). Moreover, in a recent report, Monastyrskaya et al. (*30*) used biochemical methods and immunofluorescent labeling to localize the NK-1 receptor in lipid rafts and caveolae in living cells. On this basis, it has been proposed that different lipid environments (namely, disordered and ordered lipid domains, i.e., rafts) could give rise to the ligand binding behavior observed with this receptor. Our results rule out this possibility since the distinct conformational states have been observed here in a homogeneous lipid system that does not form microdomains or separate phases at the temperatures at which the experiments were performed [i.e., 25 °C; the phase transition temperature for egg PC is −10 °C (*31*)]. It is nonetheless possible that certain receptor structural conformations may be differently partitioned into bilayer microdomains, which may explain the distinct second messenger signaling associated with the two binding sites. We have observed using PWR that the partitioning of the delta opioid receptor into microdomains is dependent on the ligand that is bound to this receptor, i.e., on its conformational state (*24*). Several other studies have reported the preferential partitioning of receptors in or out of microdomains and the influence of ligand on the partitioning (*32*, *33*).

Furthermore, our results contrast with other proposals about the NK-2 receptor where it was suggested that there is a spontaneous or agonist-induced interchange between the different conformations of the receptor (*29*, *34*). It is unlikely that the existence of the distinct conformational states of the receptor associated with the different binding sites might be associated with the receptor dimerization, inasmuch as a recent study on the homodimerization of the NK-1 receptor in living cells using fluorescence resonance energy transfer (FRET) microscopy rules out the presence of constitutive or ligand-induced homodimers or oligomers (*35*).

CONCLUSIONS

It is not clear yet what the structural basis is for the existence of these two distinct binding sites. It does not seem probable that two different ligand binding sites would exist in the same receptor molecule. Thus, the mechanism of most GPCR ligand binding and activation involves both the extracellular loops and the transmembrane helices in a complicated and coordinated process. It seems unlikely that the NK-1 receptor would have two binding sites that are so well separated in space and conformationally independent that the occupation of one does not affect the binding of ligand to the second site. This is especially true in view of the fact that photolabeling studies have shown that all these ligands share common amino acid interaction points on the NK-1 receptor (*36*−*38*). Furthermore, the fact that the maximal binding capacities for the radioligands, NK-1 agonists and septide-like molecules, are different rules out the idea that the binding sites could be located on the same molecule (*39*). One plausible explanation would be the existence of two pools of this receptor protein that do not interchange, or the existence of two isoforms of the receptor that could arise from different post-translational modification-(s) of the same gene. Although this question requires further exploration, the results presented herein do not exclude the existence of two receptor populations but do rule out the hypothesis that these two binding sites are only ligand-driven alternative tertiary conformations of a single receptor species, as described for other GPCRs (*40*, *41*).

SUPPORTING INFORMATION AVAILABLE

A SDS gel electrophoresis and western Blot analysis showing the purification of the NK-1 receptor. This material is available free of charge via the Internet at http://pubs.acs.org.

REFERENCES

1. Salamon, Z., Macleod, H. A., and Tollin, G. (1997) Coupled plasmon-waveguide resonators: A new spectroscopic tool for probing proteolipid film structure and properties, *Biophys. J. 73*, 2791−2797.
2. Tollin, G., Salamon, Z., and Hruby, V. J. (2003) Techniques: Plasmon-waveguide resonance (PWR) spectroscopy as a tool to study ligand-GPCR interactions, *Trends Pharmacol. Sci. 24*, 655−659.
3. Salamon, Z., Lindblom, G., and Tollin, G. (2003) Plasmon-waveguide resonance and impedance spectroscopy studies of the interaction between penetratin and supported lipid bilayer membranes, *Biophys. J. 84*, 1796−1807.
4. Salamon, Z., Cowell, S., Varga, E., Yamamura, H. I., Hruby, V. J., and Tollin, G. (2000) Plasmon resonance studies of agonist/antagonist binding to the human δ-opioid receptor: New structural insights into receptor−ligand interactions, *Biophys. J. 79*, 2463−2474.
5. Alves, I. D., Varga, E., Salamon, Z., Yamamura, H. I., Tollin, G., and Hruby, V. J. (2003) Direct observation of G-protein binding to the human δ-opioid receptor using plasmon-waveguide resonance spectroscopy, *J. Biol. Chem. 278*, 48890−48897.
6. Salamon, Z., and Tollin, G. (2001) Optical anisotropy in lipid bilayer membranes: Coupled plasmon-waveguide resonance measurements of molecular orientation, polarizability, and shape, *Biophys. J. 80*, 1557−1567.
7. Salamon, Z., and Tollin, G. (2001) Plasmon resonance spectroscopy: Probing molecular interactions at surfaces and interfaces, *Spectroscopy 15*, 161−175.
8. Pernow, B. (1983) Substance P, *Pharmacol. Rev. 35*, 85−141.
9. Otsuka, M., and Yoshioka, K. (1993) Neurotransmitter functions of mammalian tachykinins, *Physiol. Rev. 73*, 229−308.
10. Quartara, L., and Maggi, C. A. (1998) The tachykinin NK1 receptor. Part II: Distribution and pathophysiological roles, *Neuropeptides 32*, 1−49.
11. Kramer, M. S., Cutler, N., Feighner, J., Shrivastava, R., Carman, J., Sramek, J. J., Reines, S. A., Liu, G., Snavely, D., Wyatt-Knowles, E., Hale, J. J., Mills, S. G., MacCoss, M., Swain, C. J., Harrison, T., Hill, R. G., Hefti, F., Scolnick, E. M., Cascieri, M. A., Chicchi, G. G., Sadowski, S., Williams, A. R., Hewson, L., Smith, D., Carlson, E. J., Hargreaves, R. J., and Rupniak, N. M. J. (1998) Distinct mechanism for antidepressant activity by blockade of central substance P receptors, *Science 281*, 1640−1645.
12. Laufer, R., Gilon, C., Chorev, M., and Selinger, Z. (1986) [pGlu6,-Pro9]SP6−11, a selective agonist for the substance P P-receptor subtype, *J. Med. Chem. 29*, 1284−1288.
13. Sagan, S., Chassaing, G., Pradier, L., and Lavielle, S. (1996) Tachykinin peptides affect differently the second messenger pathways after binding to CHO-expressed human NK-1 receptors, *J. Pharmacol. Exp. Ther. 276*, 1039−1046.
14. Sagan, S., Beaujouan, J.-C., Torrens, Y., Saffroy, M., Chassaing, G., Glowinski, J., and Lavielle, S. (1997) High affinity binding of [^{3}H]propionyl-[Met(O2)11]substance P(7−11), a tritiated septide-like peptide, in Chinese hamster ovary cells expressing human neurokinin-1 receptors and in rat submandibular glands, *Mol. Pharmacol. 52*, 120−127.

15. Kim, H. R., Lavielle, S., and Sagan, S. (2003) The two NK-1 binding sites are distinguished by one radiolabelled substance P analogue, *Biochem. Biophys. Res. Commun. 306*, 725−729.
16. Macleod, H. A. (1986) *Thin Film Optical Filters*, ADAM Hilger, Bristol, U.K.
17. Salamon, Z., and Tollin, G. (2004) Graphical analysis of mass and anisotropy changes observed by plasmon-waveguide resonance spectroscopy can provide useful insights into membrane protein function, *Biophys. J. 86*, 2508−2516.
18. Mueller, P., Rudin, D. O., Tien, H. T., and Wescott, W. C. (1962) Reconstitution of cell membrane structure in vitro and its transformation into an excitable system, *Nature 194*, 979−980.
19. Gee, M. L., Healy, T. W., and White, L. R. (1990) Hydrophobicity effects in the condensation of water films in quartz, *J. Colloid Interface Sci. 83*, 6258−6262.
20. Silberzan, P., Leger, L., Auserre, D., and Benattar, J. J. (1991) Silanation of silica surfaces. A new method of constructing pure or mixed monolayers, *Langmuir 7*, 1647−1651.
21. Salamon, Z., Huang, D., Cramer, W. A., and Tollin, G. (1998) Coupled plasmon-waveguide resonance spectroscopy studies of the cytochrome b6f/plastocyanin system in supported lipid bilayer membranes, *Biophys. J. 75*, 1874−1885.
22. Sagan, S., Karoyan, P., Chassaing, G., and Lavielle, S. (1999) Further delineation of the two binding sites (R*(n)) associated with tachykinin neurokinin-1 receptors using [3-Prolinomethionine-(11)]SP analogues, *J. Biol. Chem. 274*, 23770−23776.
23. Sagan, S., Quancard, J., Lequin, O., Karoyan, P., Chassaing, G., and Lavielle, S. (2005) Conformational analysis of the C-terminal Gly-Leu-Met-NH2 tripeptide of substance P bound to the NK-1 receptor, *Chem. Biol. 12*, 555−565.
24. Alves, I. D., Salamon, Z., Hruby, V. J., and Tollin, G. (2005) Ligand modulation of lateral segregation of a G-protein-coupled receptor into lipid microdomains in sphingomyelin/phosphatidylcholine solid-supported bilayers, *Biochemistry 44*, 9168−9178.
25. Alves, I. D., Salgado, G. F., Salamon, Z., Brown, M. F., Tollin, G., and Hruby, V. J. (2005) Phosphatidylethanolamine enhances rhodopsin photoactivation and transducin binding in a solid supported lipid bilayer as determined using plasmon-waveguide resonance spectroscopy, *Biophys. J. 88*, 198−210.
26. Glowinski, J. (1995) The 'septide-sensitive' tachykinin receptor: Still an enigma, *Trends Pharmacol. Sci. 16*, 365−367.
27. Beaujouan, J. C., Torrens, Y., Saffroy, M., Kemel, M. L., and Glowinski, J. (2004) A 25 year adventure in the field of tachykinins, *Peptides 25*, 339−357.
28. Page, N. M. (2005) New challenges in the study of the mammalian tachykinins, *Peptides 26*, 1356−1368.
29. Palanche, T., Ilien, B., Zoffmann, S., Reck, M. P., Bucher, B., Edelstein, S. J., and Galzi, J. L. (2001) The neurokinin A receptor activates calcium and cAMP responses through distinct conformational states, *J. Biol. Chem. 276*, 34853−34861.
30. Monastyrskaya, K., Hostettler, A., Buergi, S., and Draeger, A. (2005) The NK1 receptor localizes to the plasma membrane microdomains, and its activation is dependent on lipid raft integrity, *J. Biol. Chem. 280*, 7135−7146.
31. Melchior, D. L., Bruggemann, E. P., and Steim, J. M. (1982) The physical state of quick-frozen membranes and lipids, *Biochim. Biophys. Acta 690*, 81−88.
32. Pike, L. J. (2003) Lipid rafts: Bringing order to chaos, *J. Lipid Res. 44*, 655−667.
33. Chini, B., and Parenti, M. (2004) G-Protein coupled receptors in lipid rafts and caveolae: How, when and why do they go there? *J. Mol. Endocrinol. 32*, 325−338.
34. Lecat, S., Bucher, B., Mely, Y., and Galzi, J. L. (2002) Mutations in the extracellular amino-terminal domain of the NK2 neurokinin receptor abolish cAMP signaling but preserve intracellular calcium responses, *J. Biol. Chem. 277*, 42034−42048.
35. Meyer, B. H., Segura, J.-M., Martinez, K. L., Hovius, R., George, N., Johnsson, K., and Vogel, H. (2006) FRET imaging reveals that functional neurokinin-1 receptors are monomeric and reside in membrane microdomains of live cells, *Proc. Natl. Acad. Sci. U.S.A. 103*, 2138−2143.
36. Lequin, O., Bolbach, G., Frank, F., Convert, O., Girault-Lagrange, S., Chassaing, G., Lavielle, S., and Sagan, S. (2002) Involvement of the second extracellular loop (E2) of the neurokinin-1 receptor in the binding of substance P. Photoaffinity labeling and modeling studies, *J. Biol. Chem. 277*, 22386−22394.
37. Bremer, A. A., Leeman, S. E., and Boyd, N. D. (2000) The common C-terminal sequences of substance P and neurokinin A contact the same region of the NK-1 receptor, *FEBS Lett. 486*, 43−48.
38. Sachon, E., Bolbach, G., Lavielle, S., Karoyan, P., and Sagan, S. (2003) Met174 side chain is the site of photoinsertion of a substance P competitive peptide antagonist photoreactive in position 8, *FEBS Lett. 544*, 45−49.
39. Kenakin, T. (1995) Agonist-receptor efficacy. II. Agonist trafficking of receptor signals, *Trends Pharmacol. Sci. 16*, 232−238.
40. Kenakin, T. (1997) Agonist-specific receptor conformations, *Trends Pharmacol. Sci. 18*, 416−417.
41. Kenakin, T. (2003) Ligand-selective receptor conformations revisited: The promise and the problem, *Trends Pharmacol. Sci. 24*, 346−354.

BI052586D